Environmentally adaptive processing for shallow ocean applications: A sequential Bayesian approach

J. V. Candy[a)]
Lawrence Livermore National Laboratory, P.O. Box 808, L-151, Livermore, California 94551, USA

(Received 28 December 2014; revised 21 June 2015; accepted 24 July 2015; published online 2 September 2015)

The shallow ocean is a changing environment primarily due to temperature variations in its upper layers directly affecting sound propagation throughout. The need to develop processors capable of tracking these changes implies a stochastic as well as an environmentally adaptive design. Bayesian techniques have evolved to enable a class of processors capable of performing in such an uncertain, nonstationary (varying statistics), non-Gaussian, variable shallow ocean environment. A solution to this problem is addressed by developing a sequential Bayesian processor capable of providing a joint solution to the modal function tracking and environmental adaptivity problem. Here, the focus is on the development of both a particle filter and an unscented Kalman filter capable of providing reasonable performance for this problem. These processors are applied to hydrophone measurements obtained from a vertical array. The adaptivity problem is attacked by allowing the modal coefficients and/or wavenumbers to be jointly estimated from the noisy measurement data along with tracking of the modal functions while simultaneously enhancing the noisy pressure-field measurements. © *2015 Acoustical Society of America*. [http://dx.doi.org/10.1121/1.4928140]

[ZJM] Pages: 1268–1281

I. INTRODUCTION

The shallow ocean is an uncertain, ever-changing, dispersive environment dominated by temperature fluctuations that alter sound propagation throughout. Environmental variations are created by these fluctuations (sound speed variations) as well as other disturbances caused by ambient, shipping, surface noise, and sensor noise such as flow and instrumentation noise. Temperature variations directly impact sound speed due to their strong interrelationship, while internal disturbances can be related to fish sounds (snapping shrimp, mammal communications). External disturbances are directly related to wind induced wave motion, shipping noise, and other surface related noises. In all, the shallow ocean is quite a hostile environment to attempt to extract meaningful information from directly without sophisticated processing techniques.[1] Modeling parametric uncertainties can also affect the processing problem. Thus, a successful processor would be required to adapt to these variations while simultaneously estimating modal functions that are necessary for such applications as detection, localization, tracking, inversion, and enhancement. A solution to this problem can be accomplished by developing a Bayesian processor capable of providing a joint solution to the modal function tracking and environmental adaptivity problem. The posterior distribution required is multimodal (multiple peaks) motivating a sequential Bayesian approach. Adaptive processing can be achieved using a recursive or equivalently sequential formulation. Sequential processing enables the realization of such a processor in order to account for changes especially in a shallow ocean. The processor tracks these variations by adjusting parameters that are capable of capturing these changes (nonstationary spatial/temporal variations) thereby mitigating them in the measured data and enhancing the signals of interest.

Sequential Bayesian processing incorporating propagation models along with their inherent environmental parameters as well as measurement and noise models offers a robust, parametrically adaptive approach to solve signal processing problems in such a nonstationary environment.[2] We address the problem of estimating or tracking modal functions in a hostile shallow ocean while jointly adjusting (adaptively) the inherent propagation model parameters.[3–13] We concentrate on this "parametrically adaptive" approach, that is, the processor that embeds an ocean acoustic model into its framework and sequentially estimates both the signals of interest as well as its embedded physical parameters.[14–16] In this way, the processor must solve the *joint* signal and parameter estimation problem. For our application, we choose the normal-mode (shallow ocean) propagation model with modal functions and pressure-field as our *signals* of interest along with two sets of *parameters* to be jointly (adaptively) estimated: the corresponding modal coefficients or horizontal wavenumbers. Therefore, the performance of the adaptive processors are investigated for two cases (individually): case (i): the adaptive modal coefficients and case (ii): the adaptive wavenumber parameters.[14–16]

More specifically, the acoustic measurements are combined with a set of model parameters usually obtained from *a priori* information or a sophisticated normal-mode simulator[18] that solves the underlying boundary value problem (BVP) to extract the initial parameters/states in order to construct the forward propagator and initialize the algorithm. The algorithms then use the incoming data to update the parameter set jointly with the acoustic signal processing task (enhancement). In the following, we define a processor

[a)]Electronic mail: candy1@llnl.gov

 0001-4966/2015/138(3)/1268/14/$30.00

whose enhanced states are the estimated modal functions. Here, we investigate the development of a model-based signal (modal function/pressure-field) enhancer that embeds a forward propagator into the processing scheme essentially mimicking previous model-based efforts that used a class of linearized processors linearized Kalman filter and extended Kalman filter (EKF).[8,14]

We are primarily interested in investigating the applicability of the "next generation" of model-based signal processing techniques, the particle filter (PF)[13] and the unscented Kalman filter (UKF)[17] with the goal of analyzing their performance on pressure-field data obtained from the well-known Hudson Canyon experiments performed on the New Jersey shelf.[11,13] A PF is a sequential Markov chain Monte Carlo Bayesian processor capable of providing reasonable performance for a multimodal (multiple peaked) distribution problem estimating a non-parametric representation of the posterior distribution.[13] On the other hand, the UKF is a processor capable of representing any unimodal (single peaked) distribution using a statistical linearization technique based on sigma points that deterministically characterize the posterior.[13]

To put this effort in perspective, similar work in this area has been accomplished previously using a classical, unimodal processor—the EKF to solve the joint estimation problem.[10,14] Both of these efforts discuss the parametrically adaptive approach using modal coefficients and wavenumbers as the unknown parameters and show that good results can be obtained for both localization[10] and parameter estimation.[15] The results of this effort demonstrates that (1) the "next generation" processors (PF and UKF) are capable of solving the joint estimation (modes, pressure-field) enhancement problem; (2) multimodal distributions result and can be mitigated by PF while the UKF is capable of at least producing reasonable estimates (as the EKF did), but not quite as good as the PF; and (3) feasible solutions to the joint state and parameter estimation can be obtained resulting in parametrically adaptive processors capable of adjusting to measured variations in the changing shallow ocean environment.

In order to construct the model-based processor (MBP), we first characterize the normal-mode model in terms of a state-space representation enabling a general framework for signal processing in Sec. II leading to the formulation of the forward propagators. The design of the MBP for a shallow ocean acoustic problem is discussed in Sec. III and the results are given in Sec. IV where we compare the performance of the PF and UKF for both the modal coefficient and wavenumber adaptivity problems. We discuss our results in Sec. V.

II. STATE-SPACE PROPAGATOR

For our ocean acoustic modal function enhancement problem, we assume a horizontally stratified ocean of depth h with a *known* horizontal source range r_s and depth z_s and that the acoustic energy from a point source can be modeled as a trapped wave governed by the Helmholtz equation.[1,18] The standard separation of variables technique and removing the time dependence leads to a set of ordinary differential equations; that is, we obtain a "depth only" representation of the wave equation which is an eigenvalue equation in z with

$$\frac{d^2}{dz^2}\phi_m(z) + \kappa_z^2(m)\phi_m(z) = 0, \quad m = 1, \ldots, M, \tag{1}$$

whose eigensolutions $\{\phi_m(z)\}$ are the so-called *modal functions* and κ_z is the vertical wavenumber in the z-direction; that is, they are a function of depth. These solutions depend on the sound speed profile $c(z)$ and the boundary conditions at the surface and bottom as well as the corresponding *dispersion* relation given by

$$\kappa^2 = \frac{\omega^2}{c^2(z)} = \kappa_r^2(m) + \kappa_z^2(m), \quad m = 1, \ldots, M, \tag{2}$$

where $\kappa_r(m)$ is the horizontal wavenumber (constant) associated with the mth mode in the r direction and ω is the harmonic source frequency.

By assuming a known horizontal source range *a priori*, we obtain a range solution given by the Hankel function, $H_0(\kappa_r r_s)$, enabling the pressure-field to be represented by

$$p(r_s, z) = \sum_{m=1}^{M} \beta_m(r_s, z_s)\phi_m(z), \tag{3}$$

where p is the acoustic pressure; ϕ_m is the mth modal function with the modal coefficient defined by

$$\beta_m(r_s, z_s) := qH_0(\kappa_r r_s)\phi_m(z_s), \tag{4}$$

for (r_s, z_s) the source position and q its amplitude.

A. State-space model

The depth-only eigen-equation can be transformed to state-space form by defining the state vector of the mth mode as

$$\underline{\phi}_m(z) := \begin{bmatrix} \phi_m(z) \\ \frac{d}{dz}\phi_m(z) \end{bmatrix} = \begin{bmatrix} \phi_{m1}(z) \\ \phi_{m2}(z) \end{bmatrix}, \tag{5}$$

leading to the state (vector) equation

$$\frac{d}{dz}\underline{\phi}_m(z) = \mathbf{A}_m(z)\underline{\phi}_m(z), \tag{6}$$

for

$$\mathbf{A}_m(z) = \begin{bmatrix} 0 & 1 \\ -\kappa_z^2(m) & 0 \end{bmatrix}. \tag{7}$$

Assuming that the ocean acoustic noise can be characterized by additive uncertainties, we can extend this deterministic state equation for the M-modes; that is, $\Phi(z) := [\underline{\phi}_1(z)|\cdots|\underline{\phi}_M(z)]^T$ leading to the following $2M$-dimensional Gauss–Markov representation of the model:

$$\frac{d}{dz}\mathbf{\Phi}(z) = \mathbf{A}(z)\mathbf{\Phi}(z) + \mathbf{w}(z), \tag{8}$$

where $\mathbf{w}(z) = [w_1\ w_2 \cdots w_{2M}]^T$ is additive, zero-mean random noise. The system matrix $\mathbf{A}(z)$ is

$$\mathbf{A}(z) = \begin{bmatrix} \mathbf{A}_1(z) & \cdots & 0 \\ \vdots & \ddots & \vdots \\ 0 & \cdots & \mathbf{A}_M(z) \end{bmatrix}, \tag{9}$$

with the overall state vector given by

$$\mathbf{\Phi}(z) = [\phi_{11}\ \phi_{12}\,|\,\phi_{21}\ \phi_{22}|\cdots|\phi_{M1}\ \phi_{M2}]^T. \tag{10}$$

This representation leads to the *measurement* equations, which we can write as

$$p(r_s, z) = \mathbf{C}^T(r_s, z_s)\mathbf{\Phi}(z) + v(z), \tag{11}$$

where

$$\mathbf{C}^T(r_s, z_s) = [\beta_1(r_s, z_s)\ 0|\cdots|\beta_M(r_s, z_s)\ 0]. \tag{12}$$

The random noise terms $\mathbf{w}(z)$ and $v(z)$ can be assumed Gaussian and zero-mean with respective covariance matrices, $\mathbf{R}_{ww}$ and R_{vv}. The measurement noise $[v(z)]$ can be used to represent the "lumped" effects of near-field acoustic noise field, flow noise on the hydrophone, and electronic noise. The modal noise ($\mathbf{w}$) can be used to represent the "lumped"uncertainty of sound speed errors, distant shipping noise, errors in the boundary conditions, sea state effects, and ocean inhomogeneities that propagate through the ocean acoustic system dynamics (normal-mode model). These assumptions, with known model parameters, lead to the optimal solution of the state estimation problem (Kalman filter).[8]

Since the array spatially samples the pressure-field discretizing depth, we choose to discretize the differential state equations using a central difference approach for improved numerical stability, that is, assuming uniformly spaced hydrophones, from Eq. (1) we have

$$\frac{d^2}{dz^2}\phi_m \approx \frac{\phi_m(z_\ell) - 2\phi_m(z_{\ell-1}) + \phi_m(z_{\ell-2})}{\Delta z_\ell^2}, \tag{13}$$

for $\Delta z_\ell := z_\ell - z_{\ell-1}$.

Applying this approximation to Eq. (1) gives

$$\phi_m(z_\ell) - 2\phi_m(z_{\ell-1}) + \phi_m(z_{\ell-2}) + \triangle z_\ell^2 \kappa_z^2(m)\phi_m(z_{\ell-1}) = 0,$$

where z_ℓ is the location of the ℓth sensor. Defining the discrete modal state vector as $\phi_m(z_\ell) := [\phi_m(z_{\ell-2})|\phi_m(z_{\ell-1})]^T$, we obtain the following set of difference equations for the mth mode

$$\begin{aligned} \phi_{m1}(z_\ell) &= \phi_{m2}(z_{\ell-1}), \\ \phi_{m2}(z_\ell) &= -\phi_{m1}(z_{\ell-1}) + (2 - \Delta z_\ell^2 \kappa_z^2(m))\phi_{m2}(z_{\ell-1}), \end{aligned} \tag{14}$$

with each of the corresponding A-submatrices now given by

$$A_m(z_\ell) = \begin{bmatrix} 0 & 1 \\ -1 & 2 - \triangle z_\ell^2 \kappa_z^2(m) \end{bmatrix}, \quad m = 1, \ldots, M, \tag{15}$$

and

$$\kappa_z^2(m) = \left(\frac{\omega^2}{c^2(z)}\right) - \kappa_r^2(m). \tag{16}$$

Substituting this model and combining *all* of the modes as in Eq. (9), the following overall *Gauss–Markov* representation of the normal-mode process and measurement is

$$\begin{aligned} \mathbf{\Phi}(z_\ell) &= \mathbf{A}(z_\ell)\mathbf{\Phi}(z_{\ell-1}) + \mathbf{w}(z_\ell), \\ p(r_s, z_\ell) &= \mathbf{C}^T(r_s, z_s)\mathbf{\Phi}(z_\ell) + v(z_\ell), \end{aligned} \tag{17}$$

and $\mathbf{\Phi}, \mathbf{w} \in \mathcal{R}^{2M\times 1}$, $p, v \in \mathcal{R}^{1\times 1}$ for $\mathbf{w} \sim \mathcal{N}(0, R_{ww})$, $v \sim \mathcal{N}(0, R_{vv})$ with $\mathbf{\Phi}(z_\ell) \sim \mathcal{N}(\bar{\Phi}(z_0), \bar{P}(z_0))$, $\mathbf{A} \in \mathcal{R}^{2M\times 2M}$, $C^T \in \mathcal{R}^{1\times 2M}$, and with "$\sim$" meaning "distributed as."

This completes the normal-mode representation of the shallow ocean in state-space form; next, we consider *augmenting* this model with unknown parameters to create a parametrically adaptive processor.

B. Augmented state-space models

The "parametrically adaptive" processor evolves from the normal-mode representation by defining parameter sets of interest. Variations in the ocean can be reflected, parametrically, in a number of ways. For instance, sound-speed variations are related to temperature changes especially in a shallow ocean environment directly impacting the corresponding dispersion relation of Eq. (2) that can be parametrically captured by the horizontal wavenumber. Besides the wavenumbers, modal variations can be reflected through the measured pressure-field relations of Eq. (3) that can be parametrically captured by the modal coefficients of Eq. (4). Therefore, we choose to use the modal coefficients as well as the horizontal wavenumbers (individually) as the parameters of interest in adapting to the changing shallow ocean environment.

1. Case (i): Modal coefficients

The modal coefficients of Eq. (4) can be used to capture modal function variations. In this case, we define the unknown *parameter vector* as

$$\theta_m(r_s, z_s) := \beta_m(r_s, z_s), \quad m = 1, \ldots, M,$$

and a new "augmented" state vector for the mth mode as

$$\Phi_m(z_\ell; \theta_m) := \Phi_m(z_\ell) = [\phi_{m1}(z_\ell)\phi_{m2}(z_\ell)\,|\,\theta_m(z_\ell)]^T.$$

With this choice of parameters (modal coefficients), the *augmented* state equations for the mth mode become

$$\begin{aligned}\phi_{m1}(z_\ell) &= \phi_{m2}(z_{\ell-1}) + w_{m1}(z_{\ell-1}),\\ \phi_{m2}(z_\ell) &= -\phi_{m1}(z_{\ell-1}) + (2 - \triangle z_\ell^2 \kappa_z^2(m))\phi_{m2}(z_{\ell-1})\\ &\quad + w_{m2}(z_{\ell-1}),\\ \theta_m(z_\ell) &= \theta_m(z_{\ell-1}) + \triangle z_\ell w_{\theta_m}(z_{\ell-1}),\end{aligned} \tag{18}$$

where we have selected a discrete *random walk* model $[\dot{\theta}_m(z) = w_{\theta_m}(z)]$ based on first differences to capture the variations of the modal coefficients with additive, zero-mean, Gaussian noise of covariance $R_{w_{\theta_m} w_{\theta_m}}$.

Note that when we augment the unknown parameters into the state vector to construct the *parametrically adaptive* processor, then we assume that they are random (walks) with our pre-computed initial values specified (initial conditions or means) and their corresponding covariances used to bound their uncertainty (2σ confidence bounds).

More succinctly, for the mth mode, we can write

$$\boldsymbol{\Phi}_m(z_\ell) = A_m(z_{\ell-1};\theta)\boldsymbol{\Phi}_m(z_{\ell-1}) + \mathbf{w}_m(z_{\ell-1}) \tag{19}$$

or expanding

$$\begin{bmatrix}\phi_m(z_\ell)\\ - - -\\ \theta_m(z_\ell)\end{bmatrix} = \left[\begin{array}{c|c} A_m(z_{\ell-1}) & 0\\ - & - - \\ 0 & 1\end{array}\right]\begin{bmatrix}\phi_m(z_{\ell-1})\\ - - -\\ \theta_m(z_{\ell-1})\end{bmatrix} + \begin{bmatrix}W_{\phi_m}(z_{\ell-1})\\ - - -\\ W_{\theta_m}(z_{\ell-1})\end{bmatrix}, \tag{20}$$

where $W_{\phi_m} \sim \mathcal{N}(0, R_{W_{\phi_m} W_{\phi_m}})$, $W_{\theta_m} \sim \mathcal{N}(0, R_{W_{\theta_m} W_{\theta_m}})$, $\phi_m(0) \sim \mathcal{N}(\bar{\phi}_m(0), R_{\phi_m\phi_m})$, $\theta_m(0) \sim \mathcal{N}(\bar{\theta}_m(0), R_{\theta_m\theta_m})$.

The corresponding nonlinear measurement model is given by

$$p(r_s, z_\ell) = \sum_{m=1}^{M} \theta_m(z_\ell)\phi_m(z_\ell) + v(z_\ell), \quad \ell = 1,\ldots,L, \tag{21}$$

with dispersion (sound-speed)

$$c(z_\ell) = \frac{\omega}{\sqrt{\kappa_z^2(m) + \kappa_r^2(m)}}, \quad m = 1,\ldots,M; \quad \ell = 1,\ldots,L. \tag{22}$$

To complete this representation, we combine all of the modes and unknown parameters and, therefore, the state transition is characterized by the underlying augmented state-space model as

$$\boldsymbol{\Phi}(z_\ell) = \mathbf{A}(z_{\ell-1};\Theta)\boldsymbol{\Phi}(z_{\ell-1}) + \mathbf{w}(z_{\ell-1}),$$

and the measurement, on the other hand, is determined from the nonlinear pressure-field measurement model,

$$p(r_s, z_\ell) = \mathbf{c}[\boldsymbol{\Phi}(z_\ell);\Theta] + v(z_\ell). \tag{23}$$

Note that for this case the pressure-field is nonlinear in the states (modal functions) and parameters (modal coefficients) since they are multiplicands and therefore lead to non-Gaussian measurements.

2. Case (ii): Horizontal wavenumbers

The horizontal wavenumbers of Eq. (2) can be used to capture sound-speed (temperature) variations. For this case, we define the unknown *parameter vector* as

$$\theta_m(z) := \kappa_r(m), \quad m = 1,\ldots,M,$$

and a new "augmented"state vector as

$$\boldsymbol{\Phi}_m(z_\ell;\theta_m) := \boldsymbol{\Phi}_m(z_\ell) = [\phi_{m1}(z_\ell)\phi_{m2}(z_\ell)|\theta_m(z_\ell)]^T.$$

With this choice of parameters (horizontal wavenumber), the augmented state equations for the mth mode become

$$\begin{aligned}\phi_{m1}(z_\ell) &= \phi_{m2}(z_{\ell-1}) + w_{m1}(z_{\ell-1}),\\ \phi_{m2}(z_\ell) &= -\phi_{m1}(z_{\ell-1}) + \left(2 - \triangle z_\ell^2\left(\frac{\omega^2}{c^2(z_\ell)} - \theta_m^2(z_{\ell-1})\right)\right)\\ &\quad \times \phi_{m2}(z_{\ell-1}) + w_{m2}(z_{\ell-1}),\\ \theta_m(z_\ell) &= \theta_m(z_{\ell-1}) + \triangle z_\ell w_{\theta_m}(z_{\ell-1}),\end{aligned} \tag{24}$$

where we have again selected a discrete *random walk* model $[\dot{\theta}_m(z) = w_{\theta_m}(z)]$ to capture the variations of the horizontal wavenumber with additive, zero-mean, Gaussian noise of covariance $R_{w_{\theta_m} w_{\theta_m}}$. Note that even though we know that theoretically the horizontal wavenumbers are constant for each mode, we incorporate this stochastic representation due to the uncertainty inherent in the measurements and the parametric model itself.

More succinctly, for the mth mode we can write

$$\boldsymbol{\Phi}_m(z_\ell) = A_m(z_{\ell-1};\theta)\boldsymbol{\Phi}_m(z_{\ell-1}) + w_m(z_{\ell-1}), \tag{25}$$

for

$$A_m(z_{\ell-1};\theta) = \left[\begin{array}{cc|c} 0 & 1 & 0\\ -1 & 2 - \triangle z_\ell^2\left(\frac{\omega^2}{c^2(z_\ell)} - \theta_m^2(z_{\ell-1})\right) & 0\\ - & - & - \\ 0 & 0 & 1\end{array}\right].$$

The corresponding measurement model is given by

$$\begin{aligned}p(r_s, z_\ell) &= \sum_{m=1}^{M} \beta_m(r_s, z_s; \theta_m(z_\ell))\phi_m(z_\ell) + v(z_\ell),\\ &\quad \ell = 1,\ldots,L,\end{aligned} \tag{26}$$

with

$$\beta_m(r_s, z_s;\theta_m) := qH_0(\theta_m(z_\ell)r_s)\phi_m(z_s), \tag{27}$$

and dispersion (sound-speed)

$$\begin{aligned}c(z_\ell;\theta_m) &= \frac{\omega}{\sqrt{\kappa_z^2(m) + \theta_m^2(z_\ell)}}, \quad m = 1,\ldots,M;\\ &\quad \ell = 1,\ldots,L.\end{aligned} \tag{28}$$

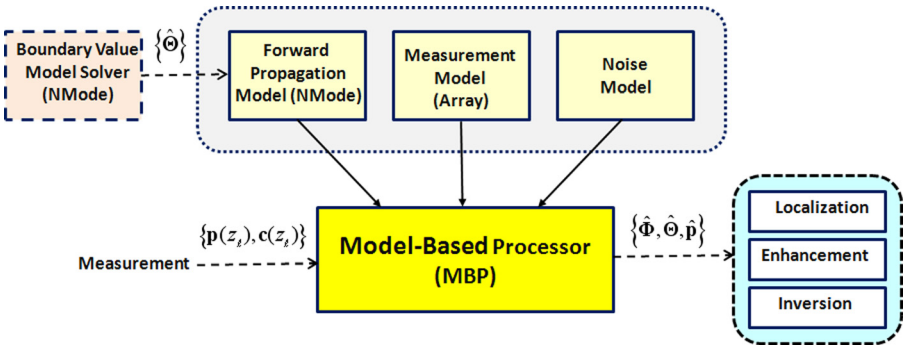

FIG. 1. (Color online) Bayesian MBP design. (a) Boundary solver for initial parameters. (b) Propagator, measurement and noise/uncertainty models. (c) MBP. (d) Applications: localization, enhancement (tracking), and inversion.

Here, the "combined" augmented model for this case leads to both a nonlinear state and measurement space, that is,

$$\begin{aligned}\mathbf{\Phi}(z_\ell;\Theta) &= \mathbf{a}[\mathbf{\Phi}(z_{\ell-1};\Theta)] + \mathbf{w}(z_{\ell-1}),\\ p(r_s,z_\ell) &= c[\mathbf{\Phi}(z_\ell;\Theta)] + v(z_\ell).\end{aligned} \tag{29}$$

In this case, both the propagator and the pressure-field measurements are nonlinear functions of the states (modes) and unknown parameters (wavenumbers). Note that the modal coefficients are also direct functions of the estimated wavenumbers and are adapted simultaneously. Therefore, this processor is clearly non-Gaussian, similar to the previous case.

It should be noted that the initial model parameters are obtained from the prior solution of the BVP typically developed as part of the experimental design process and/or after the experiment has been executed. Here, the initial "guesses" at modal coefficients and modal functions themselves are calculated based on the experimental conditions such as frequencies, current-temperature-density (CTD), archival sound-speed profiles (SSPs), boundary conditions, horizontal wavenumber estimators (e.g., see Refs. 11 and 12 for more details) to provide the input to the normal-mode BVP solutions (SNAP,[19] KRACKEN,[20] SAFARI[21]) yielding the required parameters. These parameters are then input to the state-space, measurement, and noise/uncertainty models as shown in Fig. 1.

This completes the section on the discrete state-space representation of the shallow ocean acoustic (normal-mode) propagation model that is embedded as a "forward propagator" into the subsequent processors for signal enhancement.

III. PROCESSORS

In this section, we briefly discuss the processors for our shallow oceanic problem with details available.[13] The basic adaptive problem we pursue in this paper can now be defined in terms of our mathematical models as:

GIVEN, $[\{p(r_s,\ z_\ell)\},\ \{c(z_\ell)\}]$, a set of noisy pressure-field and sound speed measurements varying in depth along with the underlying state-space model of Eqs. (25), (26) and (28) with unknown parameters $\{\theta(z_\ell)\}$, FIND the "best" (minimum error variance) estimates (joint) of the modal functions and parameters, that is, $\{\hat{\phi}_m(z_\ell)\},\{\hat{\theta}_m(z_\ell)\}$; $m=1,\ldots,M$ and measurements $\{\hat{p}(r_s,z_\ell)\}$.

The solution to this problem lies in the *joint state/parameter estimation* problem, that is, defining the *augmented state vector*,

$$\mathbf{\Phi}(z_\ell;\mathbf{\Theta}) := \begin{bmatrix}\mathbf{\Phi}(z_\ell)\\ ---\\ \mathbf{\Theta}\end{bmatrix},$$

and starting with the joint distribution applying Bayes' theorem, we obtain[13]

$$\begin{aligned}&\Pr\left[\mathbf{\Phi}(z_\ell;\mathbf{\Theta})|P_\ell\right]\\ &\quad=\left(\frac{\Pr\left[p(r_s,z_\ell)|\mathbf{\Phi}(z_\ell;\mathbf{\Theta})\right]\times\Pr\left[\mathbf{\Phi}(z_\ell;\mathbf{\Theta})|\mathbf{\Phi}(z_{\ell-1};\mathbf{\Theta})\right]}{\Pr\left[p(r_s,z_\ell)|P_{\ell-1}\right]}\right)\\ &\qquad\times\Pr\left[\mathbf{\Phi}(z_{\ell-1};\mathbf{\Theta})|P_{\ell-1}\right],\end{aligned} \tag{30}$$

where we have assumed conditional independence and defined the set of measurements as $P_\ell := \{p(r_s,z_1),\ldots,p(r_s,z_\ell)\}$.

Define the *joint weighting function* in terms of the likelihood, transition, and evidence as

$$\begin{aligned}&W(z_\ell;\mathbf{\Theta})\\ &:=\left(\frac{\Pr\left[p(r_s,z_\ell)|\mathbf{\Phi}(z_\ell;\mathbf{\Theta})\right]\times\Pr\left[\mathbf{\Phi}(z_\ell;\mathbf{\Theta})|\mathbf{\Phi}(z_{\ell-1};\mathbf{\Theta})\right]}{\Pr\left[p(r_s,z_\ell)|P_{\ell-1}\right]}\right),\end{aligned} \tag{31}$$

yielding the *sequential* Bayesian posterior distribution as

$$\Pr[\mathbf{\Phi}(z_\ell;\mathbf{\Theta})|P_\ell] = W(z_\ell;\mathbf{\Theta})\times\Pr[\mathbf{\Phi}(z_{\ell-1};\mathbf{\Theta})|P_{\ell-1}]. \tag{32}$$

The processors for our non-Gaussian problem suite are the UKF and PF. The UKF has been discussed elsewhere[8,13] in detail. Note that it is an alternative to the nonlinear or EKF processor applied successfully in many of the model-based ocean acoustic applications.[3–7] Like the EKF, the UKF is still restricted to a unimodal distribution (single peak), but that distribution need not be Gaussian. It also performs a linearization (statistical), but not of the system dynamical model, but of an inherent nonlinear vector transformation requiring "sigma points" which accurately characterize the underlying unimodal distribution. These points have been pre-calculated for the Gaussian case.[8] It has been shown that the UKF clearly outperforms the EKF and its variants (iterated EKF, higher order EKFs, etc.) and is more accurate and precise besides being much easier to implement, since Jacobian matrices are *no longer* required.

A PF is a completely different approach to nonlinear filtering in that it removes the restriction of additive Gaussian noise sources and is clearly capable of characterizing multimodal distributions. In fact, it might be easier to think of the PF as a histogram or kernel density-like estimator in the sense that it is an empirical probability mass function (PMF) that approximates the desired *posterior distribution* such that statistical inferences can easily be performed and statistics extracted directly. Here, the idea is a radical change in thinking where we attempt to develop an empirical estimation of the posterior distribution following a purely Bayesian approach using Monte Carlo (MC) sampling theory as its enabling foundation. As one might expect, the computational burden of the PF is much higher than that of the Kalman filter, since it must provide an estimate of the underlying state posterior distribution component-by-component at *each* z_ℓ-step along with the fact that the number of samples to characterize the posterior distribution is equal to the number of particles.

Here, we are concerned with the joint estimation problem consisting of setting a prior for θ and augmenting the state vector to solve the joint estimation problem as defined above in Sec. II B thereby converting the parameter estimation problem to one of optimal filtering. Thus, the PF estimates the weights required to specify the posterior distribution, empirically, that is,

$$\hat{\Pr}\left[\boldsymbol{\Phi}(z_\ell;\boldsymbol{\Theta})|P_\ell\right] \approx \frac{1}{N_p}\sum_{i=1}^{N_p}\hat{W}_i(z_\ell;\boldsymbol{\Theta}) \times \delta(\boldsymbol{\Phi}(z_\ell;\boldsymbol{\Theta}) - \boldsymbol{\Phi}_i(z_\ell;\boldsymbol{\Theta})). \tag{33}$$

The approach we chose for our problem is to estimate these weights based on the concept of importance sampling.[13] *Importance sampling* is a technique to compute statistics with respect to one distribution using random samples drawn from another. It is a method of simulating samples from a proposal or sampling (importance) distribution to be used to approximate a targeted distribution (joint posterior) by appropriate weighting. For this choice, the weighting function is defined by

$$\mathcal{W}(z_\ell;\boldsymbol{\Theta}) := \frac{\Pr\left[\boldsymbol{\Phi}(z_\ell;\boldsymbol{\Theta})|P_\ell\right]}{q\left[\boldsymbol{\Phi}(z_\ell;\boldsymbol{\Theta})|P_\ell\right]}, \tag{34}$$

where $q[\cdot]$ is the proposed sampling or *importance distribution*.

For the "sequential" case we have that the weighting function becomes[13]

$$W(z_\ell;\boldsymbol{\Theta}) = \left(\frac{\Pr\left[p(r_s,z_\ell)|\boldsymbol{\Phi}(z_\ell;\boldsymbol{\Theta})\right] \times \Pr\left[\boldsymbol{\Phi}(z_\ell;\boldsymbol{\Theta})|\boldsymbol{\Phi}(z_{\ell-1};\boldsymbol{\Theta})\right]}{q\left[\boldsymbol{\Phi}(z_\ell;\boldsymbol{\Theta})|\boldsymbol{\Phi}(z_{\ell-1};\boldsymbol{\Theta})P_\ell\right]}\right) \times W(z_{\ell-1};\boldsymbol{\Theta}). \tag{35}$$

There are a variety of PF algorithms available, each evolving by a particular choice of the sampling or importance distribution, but perhaps the simplest is the *bootstrap* technique,[13] which we apply to our problem. Here, the importance distribution is selected as the transition prior, that is,

$$q[\boldsymbol{\Phi}(z_\ell;\boldsymbol{\Theta})|\boldsymbol{\Phi}(z_{\ell-1};\boldsymbol{\Theta})P_\ell] \rightarrow \Pr[\boldsymbol{\Phi}(z_\ell;\boldsymbol{\Theta})|\boldsymbol{\Phi}(z_{\ell-1};\boldsymbol{\Theta})], \tag{36}$$

and substituting into Eq. (35) we obtain

$$\mathcal{W}(z_\ell;\boldsymbol{\Theta}) = \Pr[p(r_s,z_\ell)|\boldsymbol{\Phi}(z_\ell;\boldsymbol{\Theta})] \times \mathcal{W}(z_{\ell-1};\boldsymbol{\Theta}). \tag{37}$$

Thus, we see that once the underlying posterior is available, the estimates of important statistics can be inferred directly. For instance, the maximum *a posteriori* (MAP) estimate is simply found by locating a particular particle $\hat{\phi}_i(z_\ell)$ corresponding to the maximum of the PMF, that is,

$$\hat{\boldsymbol{\Phi}}_i(z_\ell;\boldsymbol{\Theta})_{\text{MAP}} = \max_i \hat{\Pr}[\boldsymbol{\Phi}_i(z_\ell;\boldsymbol{\Theta})|P_\ell], \tag{38}$$

while the conditional mean (CM) or, equivalently, the minimum mean-squared error (MMSE) estimate is calculated by integrating the posterior as

$$\hat{\Phi}_i(z_\ell;\Theta)_{\text{MMSE}} = \int \boldsymbol{\Phi}_i(z_\ell;\boldsymbol{\Theta}) \times \hat{\Pr}\left[\boldsymbol{\Phi}_i(z_\ell;\boldsymbol{\Theta})|\mathrm{P}_\ell\right] dz \approx \frac{1}{N_p}\sum_{i=1}^{N_p}\mathcal{W}_i(z_\ell;\boldsymbol{\Theta}) \times \boldsymbol{\Phi}_i(z_\ell;\boldsymbol{\Theta}). \tag{39}$$

For the bootstrap implementation, we need only draw noise samples from the state and parameter distributions and use the dynamic models above (normal-mode/random walk) in Eq. (25) to generate the set of particles, $\{\boldsymbol{\Phi}_i(z_\ell;\boldsymbol{\Theta})\} \rightarrow \{\boldsymbol{\Phi}_i(z_\ell),\boldsymbol{\Theta}_i(z_\ell)\}$ for $i=1,\ldots,N_p$. That is, both sets of particles are generated from the augmented models (linear/nonlinear) for each individual case (adaptive modal coefficients or adaptive wavenumbers) from

$$\boldsymbol{\Phi}_i(z_\ell;\Theta) = \begin{cases} \mathbf{A}(z_{\ell-1})\boldsymbol{\Phi}_i(z_{\ell-1}) + \mathbf{w}_i(z_{\ell-1}) & \text{[Case (i): modal coefficients]} \\ \mathbf{a}[\boldsymbol{\Phi}_i(z_{\ell-1};\Theta)] + \mathbf{w}_i(z_{\ell-1}) & \text{[Case (ii): wavenumbers]}, \end{cases} \tag{40}$$

while the likelihood is determined from the nonlinear pressure-field measurement model

$$p(r_s,z_\ell) = c[\boldsymbol{\Phi}_i(z_\ell;\Theta)] + v(z_\ell). \tag{41}$$

Assuming additive Gaussian noise the likelihood is given by

$$\Pr\left[p(r_s,z_\ell)|\mathbf{\Phi}_i(z_\ell)\right] = \frac{1}{\sqrt{2\pi R_{vv}}}\exp\left\{-\frac{1}{2R_{vv}}\left(p(r_s,z_\ell) - c[\mathbf{\Phi}_i(z_\ell;\Theta)]\right)^2\right\}. \quad (42)$$

Thus, we estimate the posterior distribution using a sequential MC approach and construct a *bootstrap PF* using the following steps:

$$\underline{\text{Initialize}}: \ \mathbf{\Phi}_i(0),\ \mathbf{w}_i \sim \mathcal{N}(0,\mathbf{R}_{ww}),\quad W_i(0) = 1/N_p;\quad i = 1,\ldots,N_p;$$

$$\underline{\text{State transition}}:$$

$$\mathbf{\Phi}_i(z_\ell;\Theta) = \begin{cases} \mathbf{A}(z_{\ell-1})\mathbf{\Phi}_i(z_{\ell-1}) + \mathbf{w}_i(z_{\ell-1}) \ \text{[Case (i)]} \\ \mathbf{a}[\mathbf{\Phi}_i(z_{\ell-1};\Theta)] + \mathbf{w}_i(z_{\ell-1}) \ \text{[Case (ii)]} \end{cases};$$

$$\underline{\text{Likelihood probability}}: \quad \Pr[p(r_s,z_\ell)|\mathbf{\Phi}_i(z_\ell)] \text{ of Eq. (42)};$$

$$\underline{\text{Weights}}:$$

$$W_i(z_\ell;\mathbf{\Theta}) = W_i(z_{\ell-1};\mathbf{\Theta}) \times \Pr[p(r_s,z_\ell)|\mathbf{\Phi}_i(z_\ell)];$$

$$\underline{\text{Normalize}}: \quad \mathcal{W}_i(z_\ell;\mathbf{\Theta}) = \frac{W_i(z_\ell;\mathbf{\Theta})}{\sum_{i=1}^{N_p} W_i(z_\ell;\mathbf{\Theta})};$$

$$\underline{\text{Resample}}: \quad \tilde{\Phi}_i(z_\ell;\mathbf{\Theta}) \Rightarrow \mathbf{\Phi}_i(z_\ell;\mathbf{\Theta});$$

$$\underline{\text{Posterior}}:$$

$$\hat{\Pr}[\mathbf{\Phi}(z_\ell;\mathbf{\Theta})|P_\ell] = \sum_{i=1}^{N_p} \mathcal{W}_i(z_\ell;\mathbf{\Theta}) \times \delta(\mathbf{\Phi}(z_\ell;\mathbf{\Theta}) - \mathbf{\Phi}_i(z_\ell;\mathbf{\Theta}));$$

and

$$\text{MAP } \underline{\text{estimate}}: \quad \hat{\Phi}_i(z_\ell;\mathbf{\Theta})_{\text{MAP}} = \max_i \hat{\Pr}[\mathbf{\Phi}_i(z_\ell;\mathbf{\Theta})|P_\ell];$$

$$\text{MMSE } \underline{\text{estimate}}:$$

$$\hat{\Phi}_i(z_\ell;\mathbf{\Theta})_{\text{MMSE}} = \frac{1}{N_p}\sum_{i=1}^{N_p} \mathcal{W}_i(z_\ell;\mathbf{\Theta})\mathbf{\Phi}_i(z_\ell;\mathbf{\Theta}).$$

A detailed flow diagram of the PF (bootstrap) algorithm is shown in Fig. 2 illustrating the prediction and update steps along with a resampling algorithm to provide convergence. More details can be found in Refs. 13 and 22–25.

IV. MODEL-BASED OCEAN ACOUSTIC PROCESSING

In this section, we discuss the development of the propagators for the Hudson Canyon experiment performed in 1988 in the Atlantic with the primary goal of investigating acoustic propagation (transmission and attenuation) using continuous wave data.[11,12] The Hudson Canyon is located off the coast of New Jersey in the area of the Atlantic Margin Coring project borehole 6010. The seismic and coring data are combined with sediment properties measured at

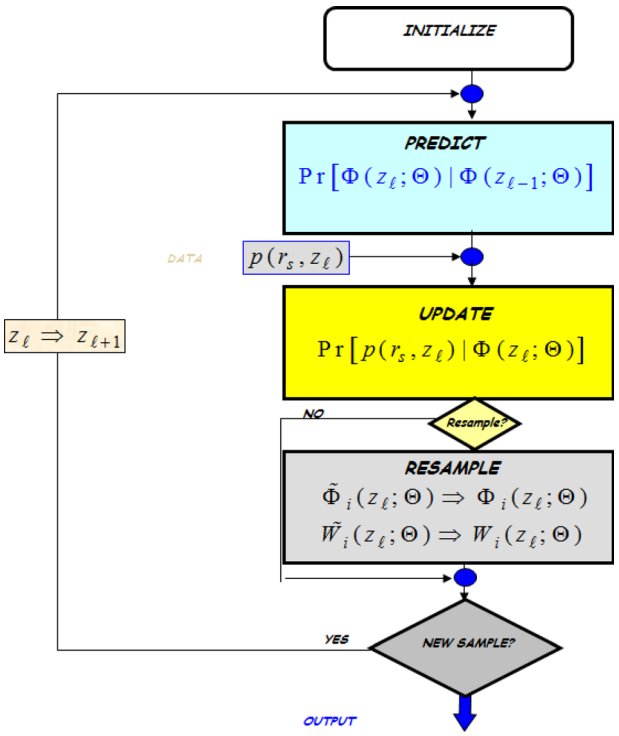

FIG. 2. (Color online) Bootstrap PF algorithm flow diagram for adaptive ocean processing: prediction, update, and resampling.

that site. Excellent agreement was determined between the model and data, indicating a well-known, well-documented shallow water experiment with bottom interaction and yielding ideal data sets for investigating the applicability of a MBP to measured ocean acoustic data. The experiment was performed at low frequencies (50–600 Hz) in shallow water of 73 m depth during a period of calm sea state as shown in Fig. 3. A calibrated acoustic source was towed at roughly 36 m depth along the 73 m isobath radially to distances of 4–26 km. The ship speed was between 2 and 4 kn. The fixed vertical hydrophone array consisted of 24 phones spaced 2.5 m apart, extending from the seafloor up to a depth of ∼14 m below the surface. The CTD and SSP measurements were made at regular intervals and the data were collected under carefully controlled conditions in the ocean environment. The normalized horizontal wavenumber spectrum for a 50 Hz temporal frequency is dominated by five modes occurring at wavenumbers between 0.14 and 0.21 m^{-1} with relative amplitudes increasing with increased wavenumber. A SNAP[19] simulation was performed and the results agree quite closely, indicating a well-understood ocean environment.

In order to construct the state-space propagator, we require the set of parameters which were obtained from the experimental measurements and processing (wavenumber spectra). The horizontal wavenumber spectra were estimated using synthetic aperture processing.[11] Eight temporal frequencies were employed: four on the inbound (75 Hz, 275 Hz, 575 Hz, 600 Hz) and four on the outbound (50 Hz, 175 Hz, 375 Hz, 425 Hz). In this application we will confine our investigation to the 50 Hz case, which is well-documented, and to horizontal ranges from 0.5 to 4 km. The

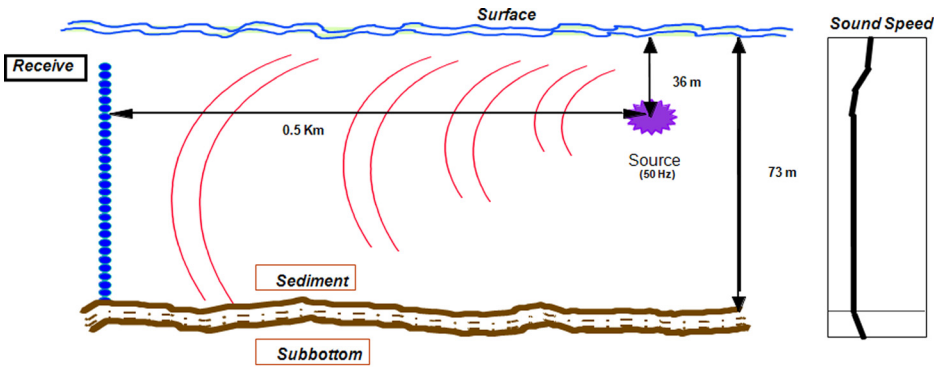

FIG. 3. (Color online) Hudson Canyon experiment geometry and structure. (a) Source at 36 m depth and 0.5 km range, 50 Hz. (b) 23-element vertical hydrophone array. (c) Five modes support the water column.

raw measured data were processed (sampled, corrected, filtered, etc.) and supplied for this investigation. We used a single snapshot of the pressure-field across the vertical array.

A. Adaptive PF design: Modal coefficients

The design and development of the environmentally adaptive PF proceeds through the following steps: (1) pre-processing the raw experimental data, (2) solving the BVP[19] to obtain initial parameter sets for each temporal frequency (e.g., modal coefficients, wavenumbers, initial conditions, etc.), (3) state-space forward propagator simulation of synthetic data for PF analysis/design, (4) application to measured data, and (5) PF performance analysis as shown in Fig. 4.

Pre-processing of the measured pressure-field data follows the usual pattern of filtering, outlier removal, and Fourier transforming to obtain the complex pressure-field as a function of depth along the array. This data along with experimental conditions (frequencies, CTD, SSPs, boundary conditions, horizontal wavenumber estimators (see Ref. 12 for details) provide the input to the normal mode BVP solutions (SNAP,[19] KRACKEN,[20] SAFARI[21]) yielding the output parameters. These parameters are then used as input to the state-space forward propagator (see Fig. 4) developed in Sec. II.

The state-space propagator is then used to develop a set of synthetic pressure-field data with higher resolution than the original raw data (e.g., 46-element array rather than 23-element at half-wave inter-element spacing). This set represents the "truth" data that can be investigated when "tuning" the PF (e.g., number of particles, covariances, etc.). Once tuned, the processors are applied directly to the measured pressure-field data (23-elements) after re-adjusting some of the processor parameters (covariances). Here, the performance metrics are estimated and processor performance analyzed. Since each run of the PF is a random realization, that is, the process noise inputs are random, an ensemble of results are estimated with its statistics presented. In this way, we can achieve a detailed analysis of the processor performance prior to fielding and operational version. In this paper, we constrain our discussion results to processing the noisy experimental pressure-field measurements.[12]

We performed a series of "tuning" runs for both the UKF and PF. We primarily adjusted the process noise covariance matrix (R_{ww}) for each of the modal functions and then executed a 100 member ensemble of realizations using these parameters. The PF was designed with the same parameters and 1500 particles were used to characterize the posterior PMF at each depth. Resampling[13] was applied at every iteration of the PF to avoid any potential degradation.

First, we investigate the enhancement capabilities of the PF in estimating the pressure-field over a 100-member ensemble shown in Fig. 5. The resulting figures show the averaged PF estimates. We observe the raw data (DATA) as well as both MAP estimates and CM estimates. Both estimators

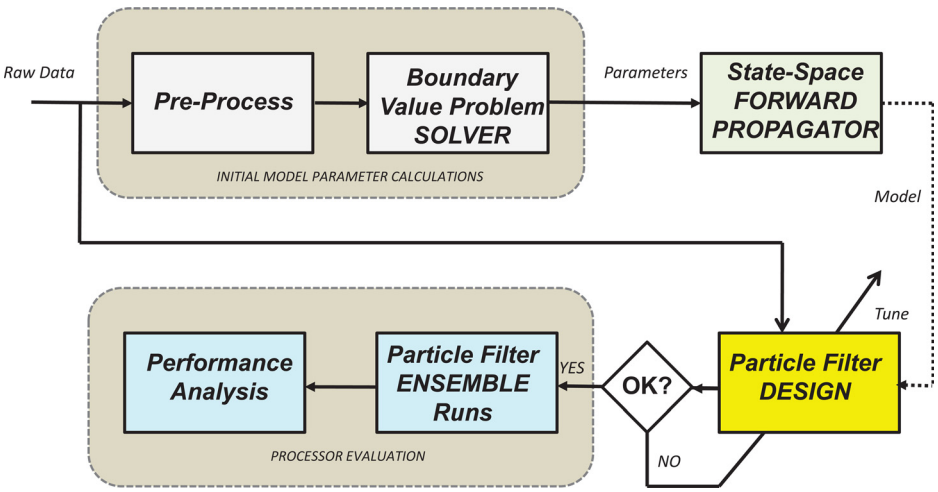

FIG. 4. (Color online) PF design/development procedure. (a) Initial parameters/conditions. (b) Design runs. (c) Ensemble runs.

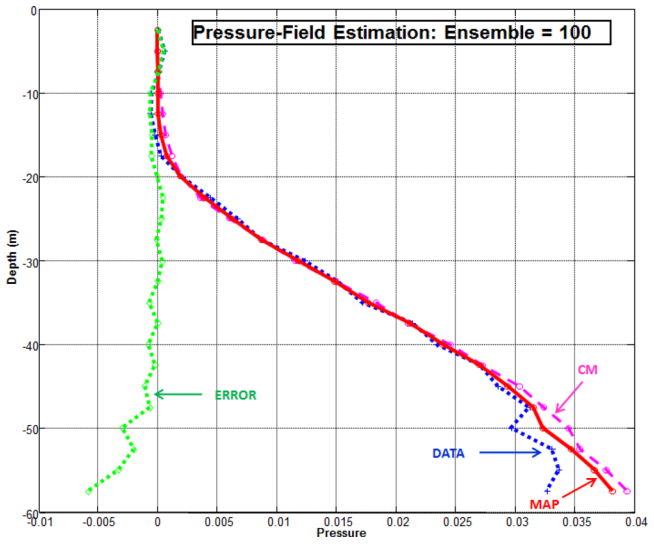

FIG. 5. (Color online) Raw/enhanced pressure-field (DATA) data from the Hudson Canyon experiment using PF estimators: MAP, CM, and the corresponding innovations (ERROR) sequence.

are capable of tracking the field quite well and even filter the erratic measurements near the bottom of the channel. The innovations or residuals (ERROR) are also shown in Fig. 5. Both estimators are capable of tracking and enhancing the pressure-field. Using classical performance metrics on the innovations sequence (ERROR), the zero-mean whiteness tests, both processors satisfy the criteria of unbiasedness (*Z-M*: $6.2 \times 10^{-4} < 4.9 \times 10^{-1}$ and uncorrelated innovations, that is, <5% exceeding the bound (6.3%). The weighted sum-squared residual (WSSR) test is also applied with satisfactory results, that is, *no* samples exceed the threshold, indicating a functionally "tuned" processor.[13] The UKF processor also produced reasonable results for the enhanced pressure-field (not shown).

Ensemble mode tracking results are shown in Figs. 6 and 7 for each of the modal function estimators, the PF (MAP/CM) and the UKF. In Fig. 6, we observe that the performance of the PF (MAP/CM) appears to track the modes quite well, especially compared to the UKF. The PF estimators perform equivalently. Two of the modal function estimates (first two) exhibit the largest errors as shown in Fig. 7, while the final three functional estimates are much better. It is interesting to note that the modal coefficient estimates are constantly being adapted (adjusted) by the processor throughout the runs, attesting to the nonstationary nature of the ocean statistics as illustrated in Fig. 8.

We also illustrate the multimodal aspect of the oceanic data by observing the modal function posterior probability mass function (PMF) estimates for modes 1 and 5 in Fig. 9.

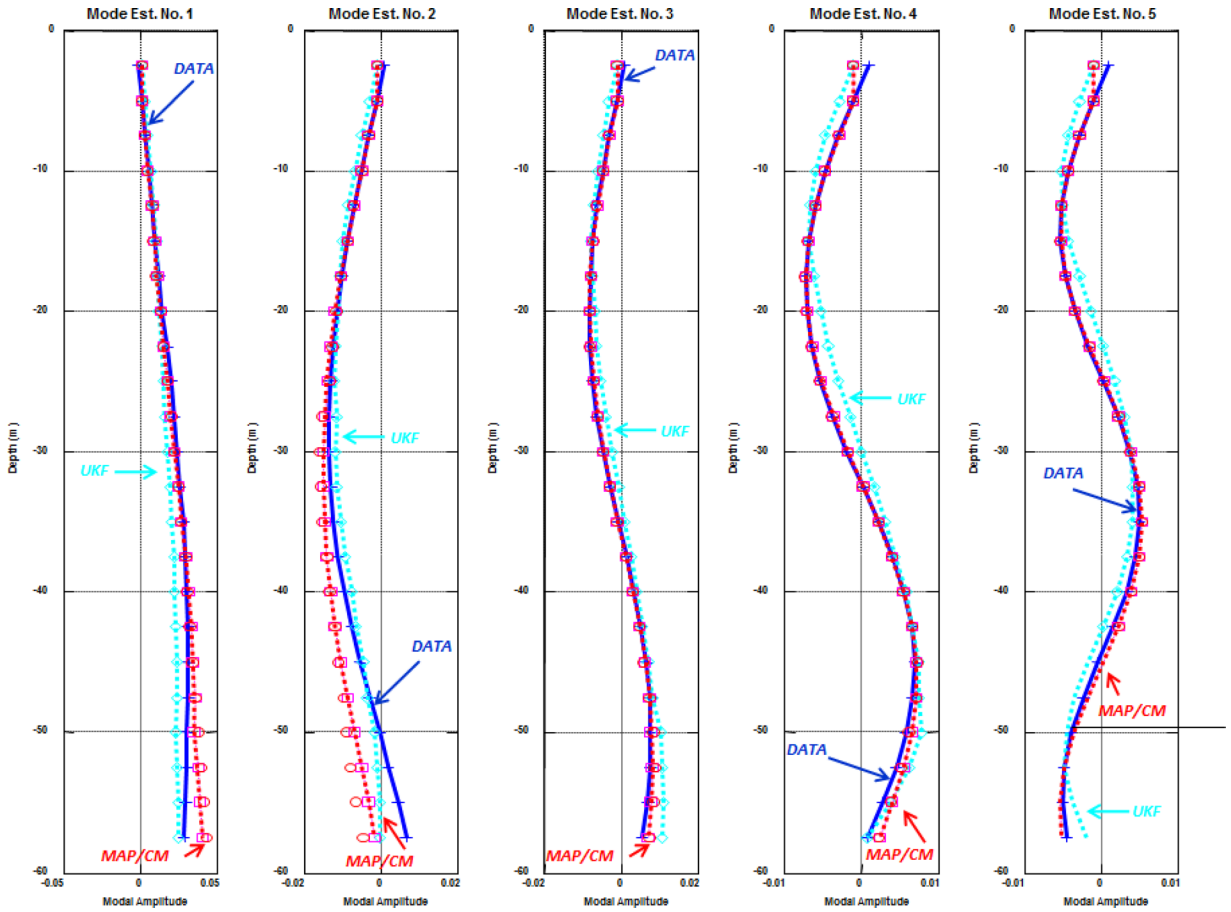

FIG. 6. (Color online) Modal function tracking for adaptive modal coefficient estimation: raw experimental data (DATA), UKF, MAP (circles) and CM (squares) PFs.

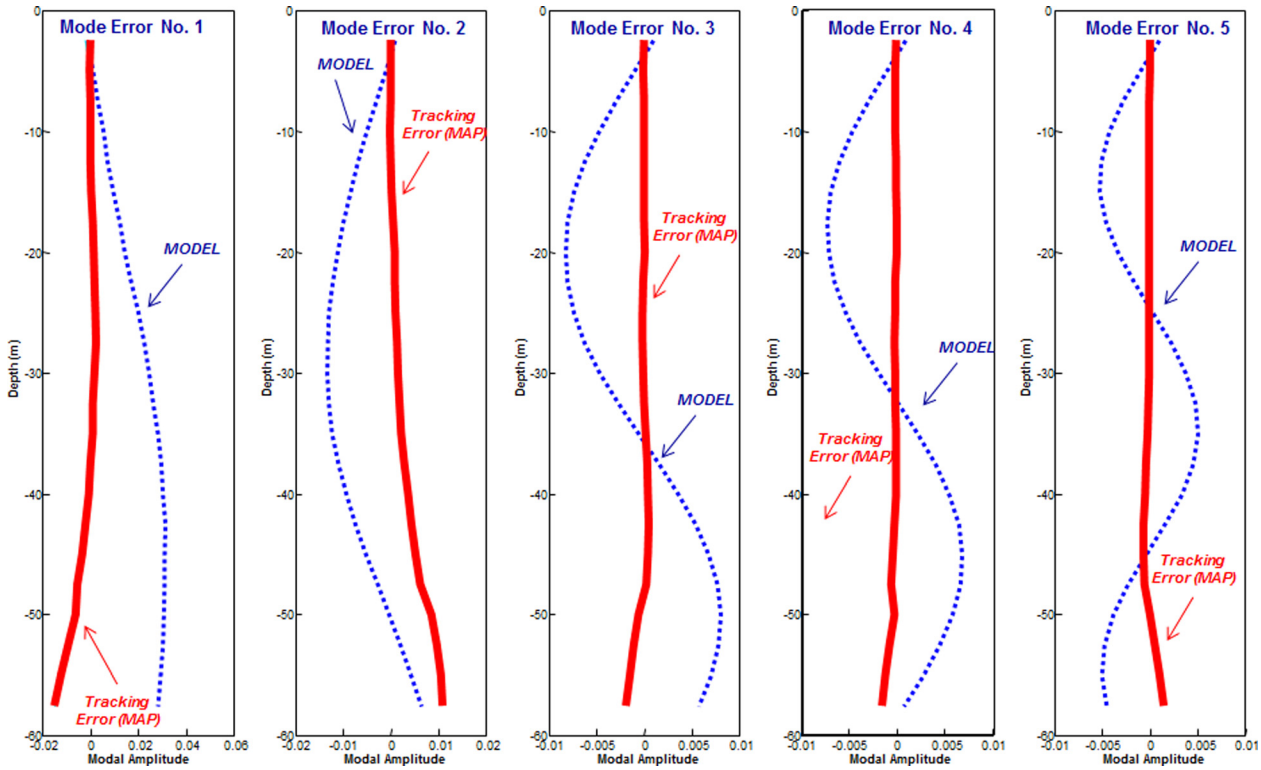

FIG. 7. (Color online) Modal function tracking errors: modal model data (Model) and MAP (tracking error) PF error.

It is clear from the plots that for each depth multiple peaks appear in the posterior estimates. The pressure-field posterior is better behaved, almost producing a near unimodal posterior for the predicted field. Visualizing a peak at each depth produces a "smooth" estimate (MAP) as shown in Fig. 10. This completes the analysis of the Hudson Canyon experimental data for the adaptive (modal coefficient) PF processing performance.

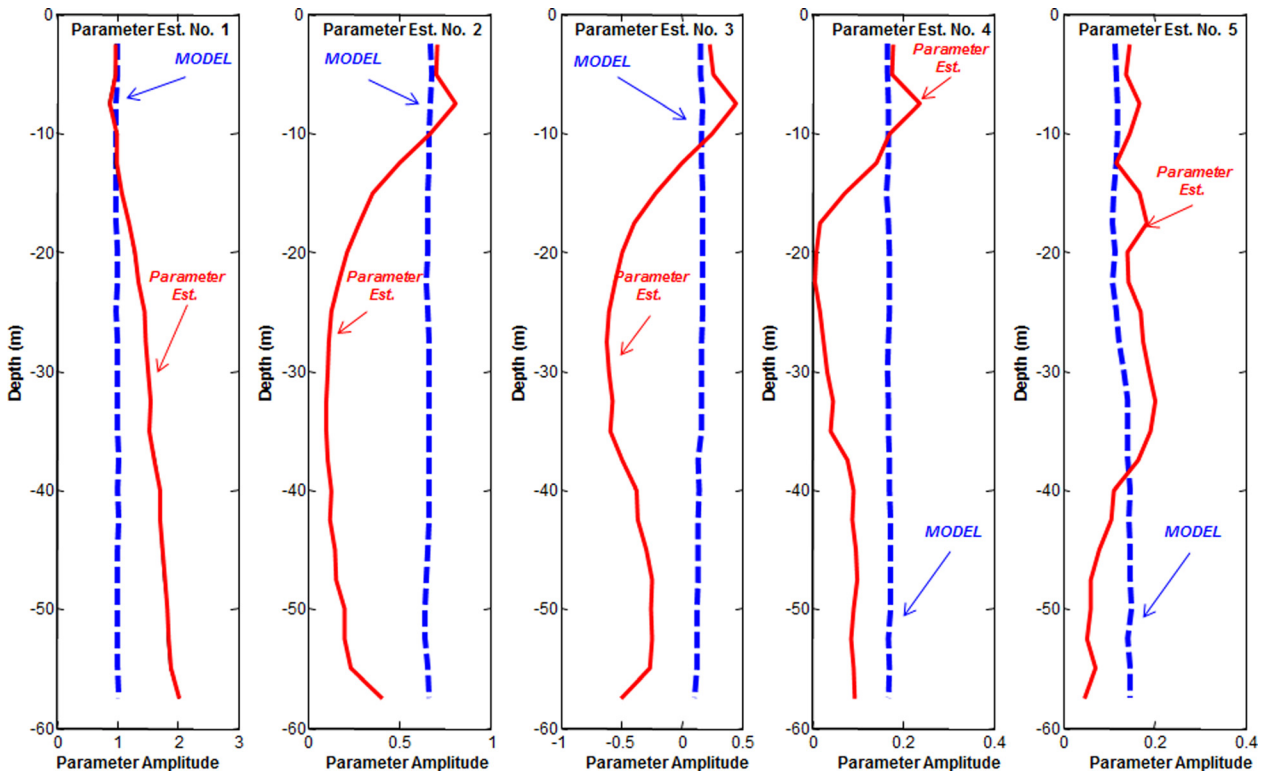

FIG. 8. (Color online) Adaptive modal coefficient parameter estimation data (MODEL) from the Hudson Canyon experiment using the MAP PF (parameter estimate).

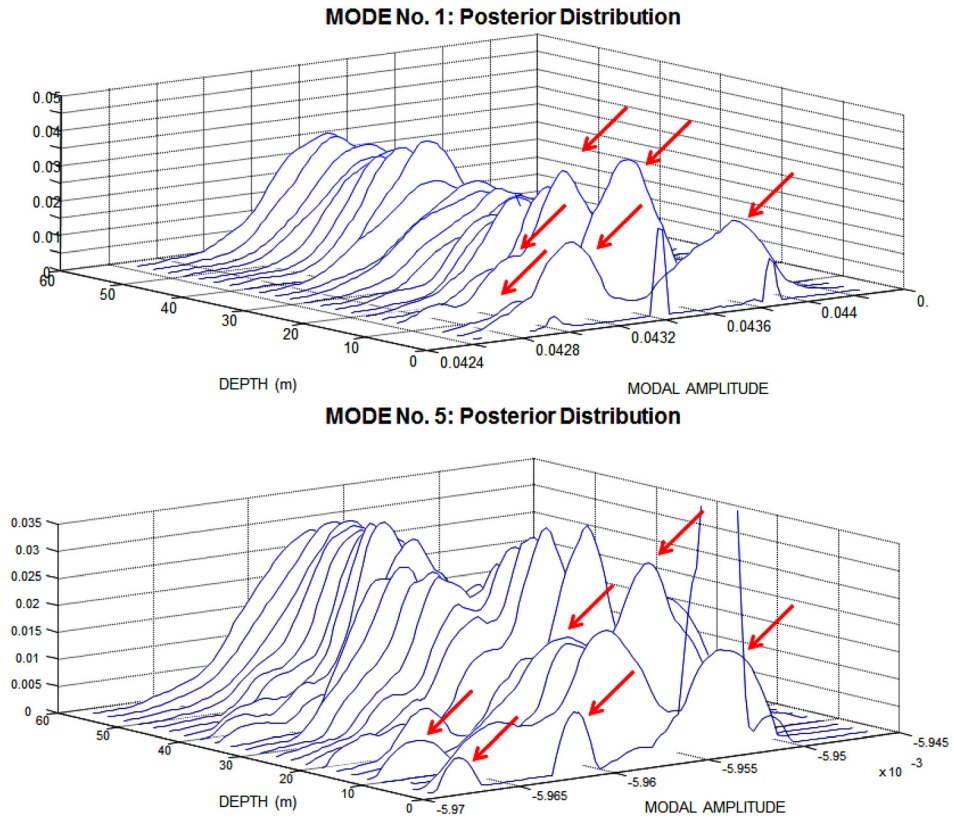

FIG. 9. (Color online) PMF posterior estimation (modes 1 and 5) surfaces for experimental Hudson Canyon data (particle vs time vs probability).

B. Adaptive PF design: Wavenumbers

As before in the modal coefficient case, we investigate the enhancement capabilities of the PF in estimating the pressure-field over a 100-member ensemble shown in Fig. 11. Using 1500-particles, we see the raw hydrophone data (dashed line) from the experiment as well as both MAP estimates (circles) and CM estimates (dotted line with circles). Both estimators appear to track the field quite well. The corresponding innovations (residual) sequence is also shown (diamonds). Classically, both estimators produced satisfactory zero-mean/statistical whiteness tests as well as the WSSR tests, indicating a "tuned" processor.[8]

The ensemble mode tracking results are shown in Fig. 12 for each of the modal function estimators, the PF (MAP/CM) and the UKF. In Fig. 12, we observe that the performance of the PF (MAP/CM) appears to track the modes quite well and better than the UKF. The PF estimators perform equivalently.

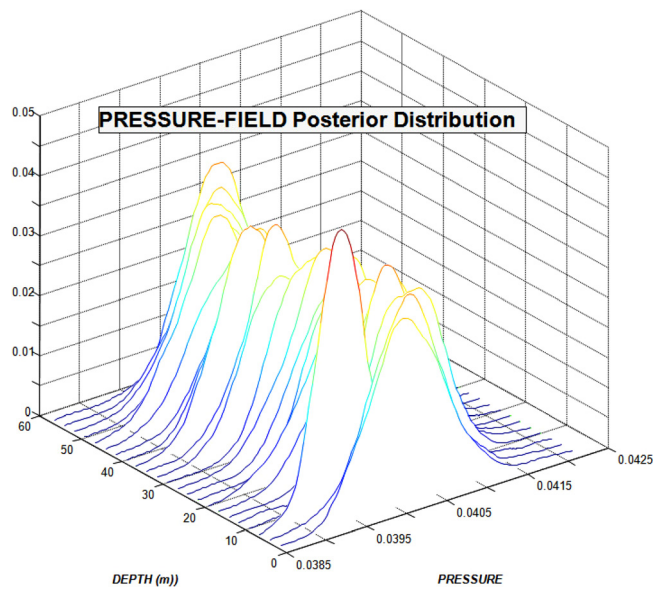

FIG. 10. (Color online) Pressure-field PMF estimation surface for experimental Hudson Canyon data (particle vs time vs probability).

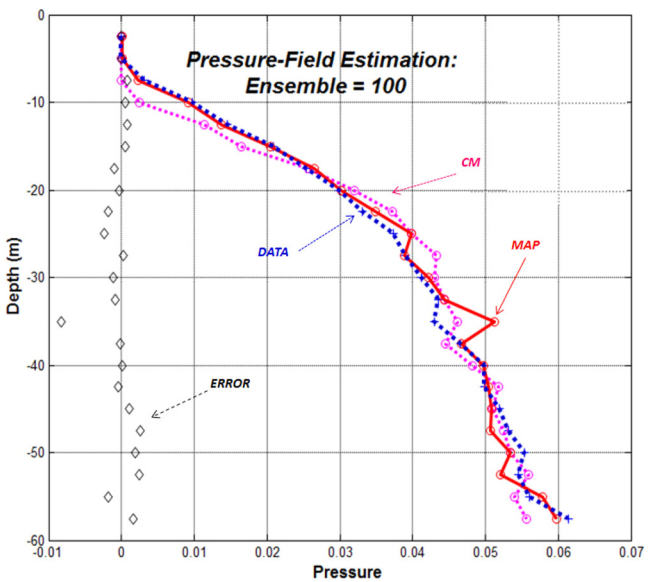

FIG. 11. (Color online) Raw pressure-field data/enhanced data (DATA) from the Hudson Canyon experiment with a 23-element hydrophone vertical array using PF estimators: MAP, CM, and the corresponding innovations (ERROR) sequence.

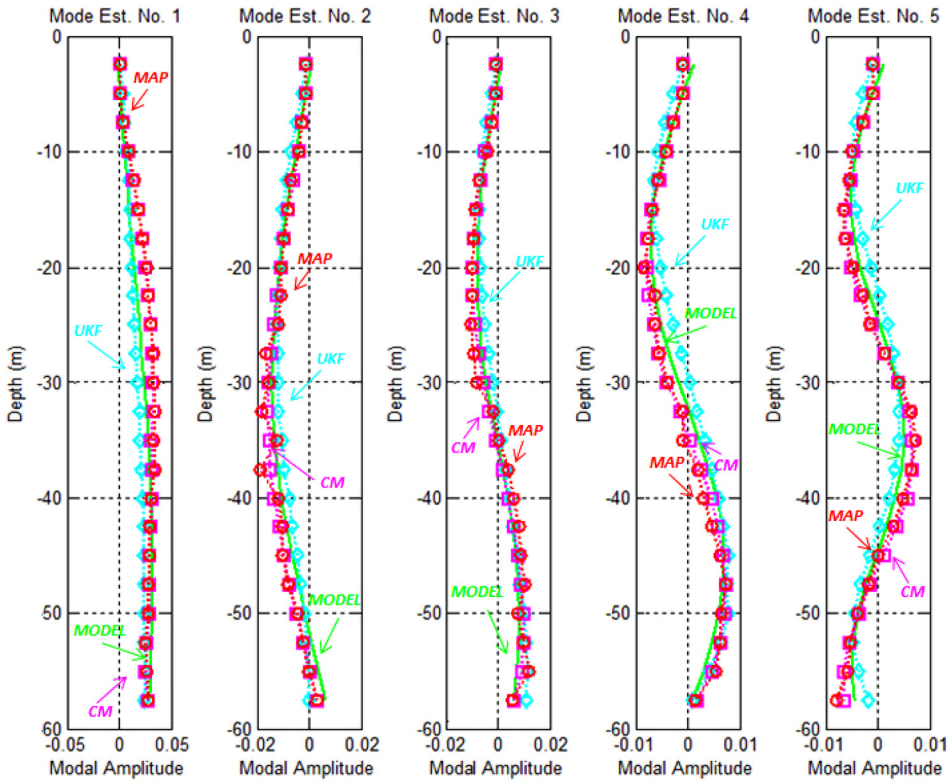

FIG. 12. (Color online) Modal function tracking for adaptive wavenumber estimation: Hudson Canyon data (MODEL) of a 23-element array, UKF, MAP, and CM (squares) PFs.

Two of the modal function estimates (first two) exhibit the largest errors while the final three functional estimates are much better. The root-mean-squared (modal tracking) error for each mode is quite reasonable on the order of 10^{-5}, again confirming their performance. It is interesting to note that the wavenumber estimates are constantly being adapted (adjusted) by the processor throughout the runs, attesting to the nonstationary nature of the ocean statistics. The ensemble

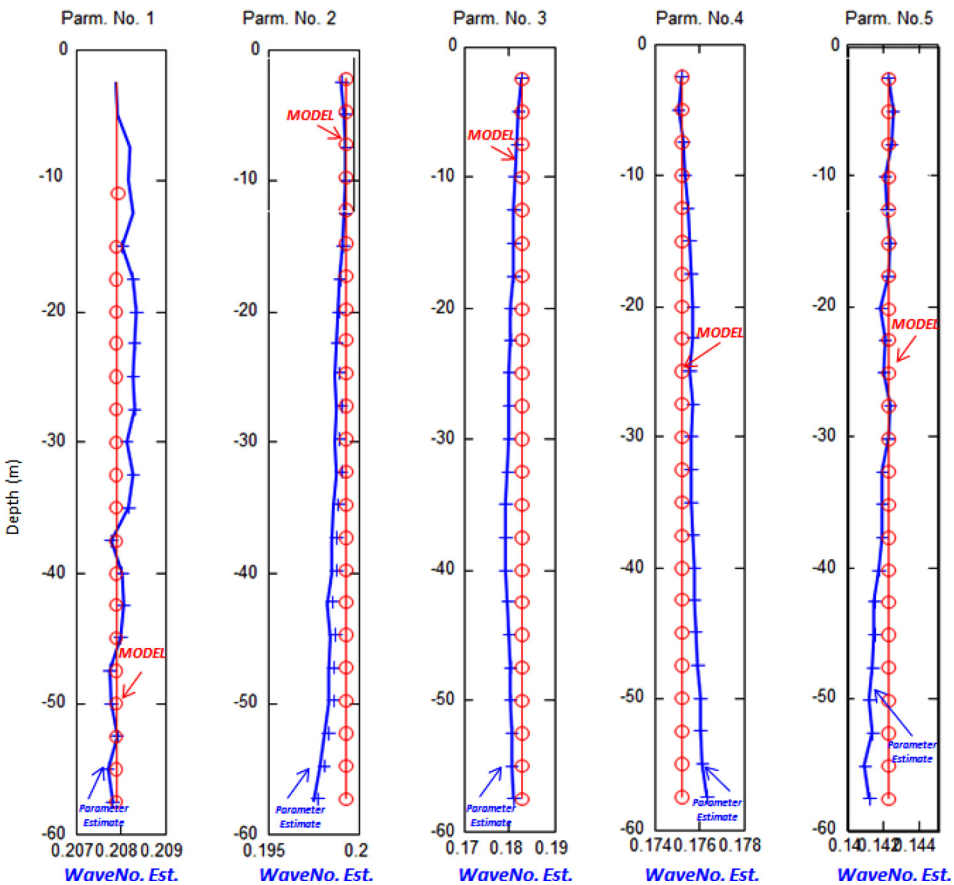

FIG. 13. (Color online) Adaptive wavenumber parameter estimates (parameter estimate) from the Hudson Canyon 23-element array data (MODEL) using the MAP PF.

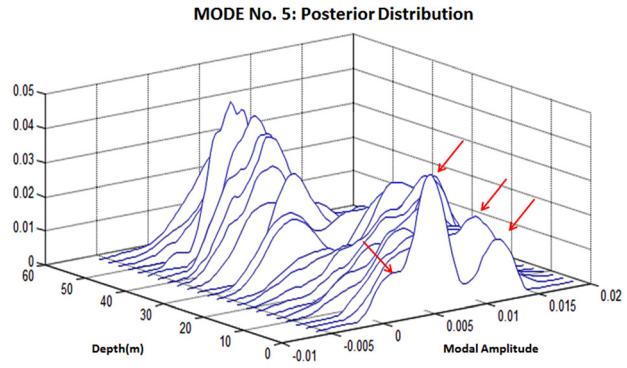

FIG. 14. (Color online) PMF posterior estimation (mode 5) surface for Hudson Canyon 23-element array data (particle vs time vs probability).

average wavenumber estimates are very reasonable: [0.206, 0.197, 0.181, 0.173, 0.142; (TRUE) 0.208, 0.199, 0.183, 0.175, 0.142]. The PF and CM ensemble estimates are very close to the true values adapting to the changing ocean environment, yet, still preserving wavenumber values on the average. On a single realization, the processors were capable of predicting the correct values, but the ensemble results give a better overall performance metric.

We also illustrate the multimodal aspect of the oceanic data by observing the modal function posterior probability PMF estimates for mode 5 illustrated in Fig. 13. It is clear from the plots that for each depth multiple peaks appear in the posterior estimates. The wavenumber PMF estimate corresponding to corresponding to mode 5 is shown in Fig. 14. Again, we note the multiple, well-defined peaks in the posterior distribution leading to the MAP parameter estimate.

The pressure-field posterior peaks over the span of the water column are illustrated. Visualizing a peak at each depth produces a "smooth" estimate (MAP) as shown in Figs. 15 and 16. This completes the analysis of the synthesized Hudson Canyon experiment and the PF processing performance.

This completes the analysis of the performance of the adaptive PF for both the modal coefficients and

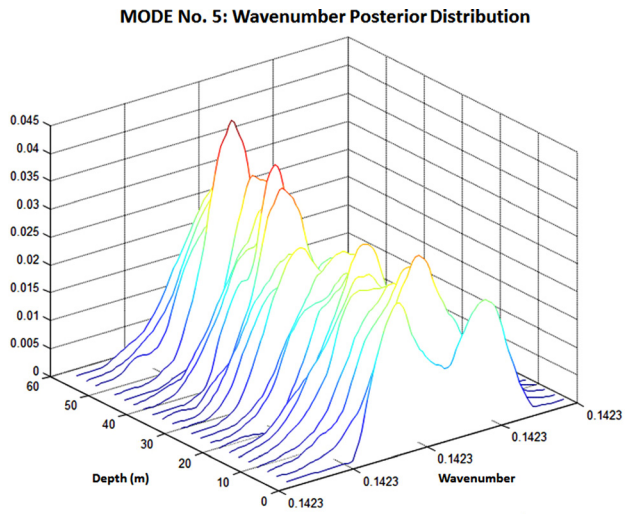

FIG. 15. (Color online) PMF posterior estimation (wavenumber 5) surface for Hudson Canyon 23-element array data (particle vs time vs probability).

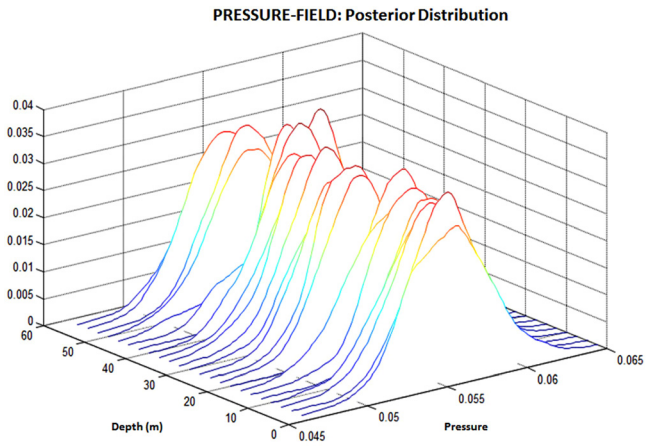

FIG. 16. (Color online) Pressure-field posterior PMF estimation surface for Hudson Canyon data (particle vs time vs probability).

wavenumbers. It is clear from these ensemble runs that the PF is capable of parametrically adapting to the changing shallow ocean environment in both these cases, providing reasonable tracking estimates of the modal functions while simultaneously estimating the associated pressure-field and unknown parameters.

V. SUMMARY

In this paper, we have discussed the development of environmentally adaptive processors capable of tracking modes and enhancing the raw pressure-field measurements obtained from a vertical hydrophone array in shallow water. The parametric adaption was based on simultaneously estimating either the modal coefficients or the horizontal wavenumbers along with the modes and pressure-field as the environmental parameters of interest. These wavenumber parameters were more challenging from a processor design perspective because of their increased sensitivity to environmental change compared to the modal coefficients. We chose a Bayesian sequential design because of the varying nature of the shallow ocean and applied a normal-mode model in state-space form to create a forward propagator. The algorithms applied were the UKF and the PF, both modern approaches applied to this problem. We compared their performance and found slightly better results for the PF over a 100-member ensemble.

Much more effort must be applied to gain a full understanding of applying these approaches to usual ocean acoustic problems (localization, tracking, inversion, etc.). Our future efforts will be focused on extending the processors to those problems.

ACKNOWLEDGMENTS

This work was performed under the auspices of the U.S. Department of Energy by Lawrence Livermore National Laboratory under Contract No. DE-AC52-07NA27344.

[1]C. S. Clay and H. Medwin, *Acoustical Oceanography* (Wiley, New York,1977), pp. 1–544.

[2]C. Yardim, Z-H. Michalopoulou, and P. Gerstoft, "An overview of sequential Bayesian filtering in ocean acoustics," IEEE J. Oceanic Eng. **36**(1), 71–89 (2011).
[3]M. J. Hinich, "Maximum likelihood signal processing for a vertical array," J. Acoust. Soc. Am. **54**, 499–503 (1973).
[4]C. S. Clay, "Use of arrays for acoustic transmission in a noisy ocean," Res. Geophys. **4**(4), 475–507 (1966).
[5]H. P. Bucker, "Use of calculated sound fields and matched-field detection to locate sound sources in shallow water," J. Acoust. Soc. Am. **59**, 368–373 (1976).
[6]A. M. Richardson and L. W. Note, "*A posteriori* probability source localization in an uncertain sound speed, deep ocean environment," J. Acoust. Soc. Am. **89**(6), 2280–2284 (1991).
[7]E. J. Sullivan and D. Middleton, "Estimation and detection issues in matched-field processing," IEEE J. Oceanic Eng. **18**(3), 156–167 (1993).
[8]J. V. Candy, *Model-Based Signal Processing* (Wiley/IEEE, Hoboken, NJ, 2006), pp. 1–677.
[9]J. V. Candy and E. J. Sullivan. "Ocean acoustic signal processing: A model-based approach," J. Acoust. Soc. Am. **92**(12), 3185–3201 (1992).
[10]J. V. Candy and E. J. Sullivan, "Passive localization in ocean acoustics: A model-based approach," J. Acoust. Soc. Am. **98**(3), 1455–1471 (1995).
[11]W. M. Carey, J. Doutt, R. Evans, and L. Dillman, "Shallow water transmission measurements taken on the New Jersey continental shelf," IEEE J. Oceanic Eng. **20**(4), 321–336 (1995).
[12]A. R. Rogers, Y. Yamamoto, and W. Carey, "Experimental investigation of sediment effect on acoustic wave propagation in shallow water," J. Acoust. Soc. Am. **93**, 1747–1761 (1993).
[13]J. V. Candy, *Bayesian Signal Processing: Classical, Modern and Particle Filtering Methods* (Wiley/IEEE, Hoboken, NJ, 2009), pp. 1–445.
[14]J. V. Candy and E. J. Sullivan, "Model-based identification: An adaptive approach to ocean-acoustic processing," IEEE J. Ocean. Eng. **21**(3), 273–289 (1996).
[15]J. V. Candy, "An adaptive particle filtering approach to tracking modes in a varying shallow ocean environment," in *Proc. OCEANS'11*, Santander, Spain (2011), pp. 1–10.
[16]J. V. Candy, "Parametrically adaptive wavenumber processing for mode tracking in a shallow ocean environment," in *Proc. OCEANS'12*, Hampton Beach, VA (2012), pp. 1–6.
[17]S. Haykin and N. de Freitas, "Special issue: Sequential state estimation: From Kalman filters to particle filters," Proc. IEEE **92**(3), 399–574 (2004).
[18]F. B. Jensen, W. A. Kuperman, M. B. Porter, and H. Schmidt, *Computational Ocean Acoustics* (AIP, New York, 1994), pp. 1–455.
[19]F. B. Jensen and M. C. Ferla, "SNAP: The SACLANTCEN normal-model propagation model," Report SM-121, SACLANTCEN, Italy (1979), pp. 1–177.
[20]M. B. Porter, "The KRACKEN normal mode program," Report SM-245, SACLANTCEN, Italy (1991), pp. 1–183.
[21]H. Schmidt, "SAFARI: Seismo-acoustic fast field algorithm for range independent environments," Report SM-245, SACLANTCEN, Italy (1987), pp. 1–142.
[22]B. Ristic, S. Arulampalam, and N. Gordon, *Beyond the Kalman Filter: Particle Filters for Tracking Applications* (Artech House, Boston, 2004), pp. 1–309.
[23]O. Cappe, E. Moulines, and T. Ryden, *Inference in Hidden Markov Models* (Springer, New York, 2005), pp. 1–650.
[24]S. Godsill and P. Djuric, "Special issue: Monte Carlo methods for statistical signal processing," IEEE Trans. Signal Proc. **50**, 1–423 (2002).
[25]P. Djuric, J. Kotecha, J. Zhang, Y. Huang, T. Ghirmai, M. Bugallo, and J. Miguez, "Particle filtering," IEEE Signal Proc. Mag. **20**(5), 19–38 (2003).